Characterizing distortion-product otoacoustic emission components across four species

Glen K. Martin,[a] Barden B. Stagner, You Sun Chung, and Brenda L. Lonsbury-Martin
Research Service, VA Loma Linda Healthcare System and Department of Otolaryngology–Head and Neck Surgery, Loma Linda University Medical Center, Loma Linda, California 92357

(Received 14 October 2010; revised 31 January 2011; accepted 8 February 2011)

Distortion-product otoacoustic emissions (DPOAEs) were measured as level/phase (L/P) maps in humans, rabbits, chinchillas, and rats with and without an interference tone (IT) placed either near the $2f_1-f_2$ DPOAE frequency place (f_{dp}) or at one-third of an octave above the f_2 primary tone (1/3-oct IT). Vector differences between with and without IT conditions were computed to derive a residual composed of the DPOAE components removed by the IT. In humans, a DPOAE component could be extracted with the expected steep phase gradient indicative of reflection emissions by ITs near f_{dp}. In the laboratory species, ITs near f_{dp} failed to produce any conclusive evidence for reflection components. For all species, 1/3-oct ITs extracted large DPOAE components presumably generated at or basal to the IT-frequency place that exhibited both distortion- and reflection-like phase properties. Together, these findings suggested that basal distortion components could assume reflection-like phase behavior when the assumptions of cochlear-scaling symmetry, the basis for shallow phase gradients for constant f_2/f_1 ratio sweeps, are violated. The present results contradict the common belief that DPOAE components associated with steep or shallow phase slopes are unique signatures for reflection emissions arising from f_{dp} or distortion emissions generated near f_2, respectively. © *2011 Acoustical Society of America*. [DOI: 10.1121/1.3560123]

PACS number(s): 43.64.Bt, 43.64.Jb, 43.64.Kc [WPS] Pages: 3090–3103

NOMENCLATURE

BM	basilar membrane
DP-gram	DPOAE level as a function of the f_2 primary-tone frequencies
DPOAE	distortion-product otoacoustic emission
DSP	digital signal processor
f_1, f_2	lower- and upper-frequency primary tones, respectively
f_2/f_1	ratio describing the frequency separation of f_1 and f_2
f_{dp}	distortion-product frequency place
FFT	fast Fourier transform
IT	interference tone
L/P	level/phase map
L_1, L_2	level of f_1 and f_2, respectively
NF	noise floor
OHC	outer hair cell
oct	octave
SFOAE	stimulus frequency otoacoustic emission
TW	traveling wave

I. INTRODUCTION

A well-established concept in the otoacoustic emissions (OAEs) literature is that the generation of distortion-product otoacoustic emissions (DPOAEs), especially in humans, is adequately described by a two-source model (e.g., Shera and Guinan 1999; Talmadge *et al.*, 1999; Knight and Kemp 2000, 2001; Kalluri and Shera, 2001; Konrad-Martin *et al.*, 2001; Dhar *et al.*, 2005). In this formulation, one source is thought to arise from the nonlinear interactions between the f_1 and f_2 primary tones, near the peak of the f_2 traveling wave (TW). Shera and Guinan (1999) referred to this constituent as the "generator" or "distortion" component, while Knight and Kemp (2000) described it as a "wave-fixed" component. This component is thought to travel both apically and basally within the cochlea. When the apically traveling segment arrives at the $2f_1-f_2$ DPOAE frequency place (f_{dp}) on the basilar membrane (BM), a second component, which is presumably generated by a coherent-reflection mechanism, travels basally to produce another DPOAE source referred to as the "reflection component" (Shera and Guinan, 1999), or a "place-fixed" component (Knight and Kemp, 2000). Thus, the prevailing view is that lower-sideband DPOAEs (e.g., $2f_1-f_2$) conform to a two-source model with the emissions arising from two discrete locations associated with distinct mechanisms of generation.

These two generation mechanisms are thought to be associated with characteristic phase behaviors. The so-called distortion source exhibits shallow phase gradients as a function of DPOAE frequency due to cochlear-scaling symmetry (Zweig and Shera, 1995; Shera and Guinan, 1999; Shera *et al.*, 2000). This scaling factor results in horizontal phase banding in DPOAE level/phase (L/P) maps when DPOAE phase is plotted as a function of the DPOAE frequency with the f_2/f_1 ratio held constant (e.g., Knight and Kemp, 2000, 2001; Martin *et al.*, 2009, 2010a,b). In contrast, the reflection source exhibits steep phase gradients because, as the primary tones are swept, successively different "reflection" regions are encountered as a function of f_{dp}, and consequently,

[a]Author to whom correspondence should be addressed. Electronic mail: glen.martin2@va.gov

 0001-4966/2011/129(5)/3090/14/$30.00

DPOAE phase varies rapidly. This property presumably results in vertical phase banding in DPOAE L/P maps.

Recently, by using interference tones (ITs) in human subjects to manipulate their DPOAE L/P maps, Martin *et al.* (2009) presented evidence that questioned the above assumptions that DPOAEs with steep phase slopes arise exclusively from near f_{dp}, and that those with shallow slopes arise primarily from near the peak of the f_2 TW. In the Martin *et al.* (2009) study, to remove the reflection component, DPOAE L/P maps were obtained with and without an IT placed near f_{dp}. Vector differences computed between these two conditions revealed the reflection component to be a small patchy "residual" accompanied by narrow vertical phase bands representing the DPOAE components "taken away" by the IT. However, DPOAE L/P maps measured in the presence of the IT still contained significant regions where DPOAEs with vertical phase banding remained. By placing an IT 1/3 octave above f_2 (i.e., 1/3-oct IT), these DPOAEs accompanied by vertical banding could be removed thus inferring that they represented basal DPOAE components. In the resulting residuals, these emissions as well as a significant component with horizontal banding at wider f_2/f_1 ratios could be readily visualized. Such emission components presumably make up part of a distributed source of DPOAEs generated at and above the 1/3-oct IT frequency place in the tails of the primary-tone TWs, especially at the higher primary-tone levels necessary to acquire DPOAE L/P maps from humans.

The above findings in humans were further elaborated upon in subsequent experiments in both normal and noise-damaged rabbit subjects (Martin *et al.*, 2010a,b). In normal rabbit ears, essentially no reflection components were extracted by ITs near f_{dp}. Thus, in this species, vertical phase banding in the DPOAE L/P maps was not attributed in any part to a reflection component from f_{dp}. As in humans, a 1/3-oct IT removed most $2f_1-f_2$ DPOAEs with vertical phase banding characteristics at narrow f_2/f_1 ratios, along with most of the $2f_2-f_1$ DPOAEs as well. At wider f_2/f_1 ratios in normal rabbit ears, again as in humans the residual also contained appreciable $2f_1-f_2$ DPOAE components with horizontal phase banding. Further studies in rabbit ears with restricted noise-induced lesions ruled out the effects of the IT on primary-tone levels, or possible catalyst effects (see Fahey *et al.*, 2000), as alternate explanations for the apparent basal source of DPOAEs. To summarize, the rabbit findings (Martin *et al.*, 2010a,b) convincingly demonstrated the presence of DPOAE components arising basal to the 1/3-oct IT that exhibited either distortion- or reflection-like phase characteristics.

The present study replicates the above findings of basal DPOAE components in normal human and rabbit ears and extends the results to chinchilla and rat subjects. The results presented below establish the generality of the above outcomes, and demonstrate that they are in no way unique to rabbits, but are a characteristic of DPOAEs in both humans and in some common laboratory species. Thus, the normal ears of all four species exhibited vertical phase banding in DPOAE L/P maps that was not removed by ITs near f_{dp}. Such DPOAE components were, however, substantially reduced or removed by a 1/3-oct IT, again strongly implicating a region at or above the IT-frequency place as their source of origin. At or near "optimal" f_2/f_1 ratios, all four species also revealed residual DPOAE components with horizontal phase banding that seemed to originate from basal cochlear locations. Overall, the present results establish the presence of substantial basal DPOAE components in both humans and in some common laboratory animal species.

II. METHODS

A. Subjects

Ten normal-hearing humans ($n=5$ male, $n=5$ female), and several representatives of three other species [$n=4$ female rabbits (3–4 kg); $n=2$ female chinchillas (400–500 g); $n=2$ male rats (300–400 g)] served as experimental subjects. Human subjects (mean age $=28.6\pm5.25$ yr) demonstrated normal-hearing levels bilaterally of $\leq$10 dB HL at all standard audiometric test frequencies, at octave intervals between 0.250 and 8 kHz, along with normal DPOAEs compared to our laboratory's human database. In addition, rabbit subjects showed normal cochlear function in both ears as measured by DPOAE level as a function of the f_2 primary-tone frequencies (DP-grams), which were comparable to those in our laboratory's extensive normative rabbit DPOAE database. The chinchillas and rats had robust DPOAEs, but no other measures were performed to confirm their hearing status.

DPOAE testing for the human subjects and the three laboratory species was performed in a sound-attenuated chamber. Humans were tested while seated in a reclining lounge chair. Rabbits were first habituated to being confined in a standard Plexiglas rabbit holder (Plas Labs, Lansing, MI) and were tested while awake. Chinchillas were tested while anesthetized by 2.0%–2.5% isoflurane inhalation anesthesia, whereas rats were examined while anesthetized by an intramuscular injection of ketamine (44 mg/kg) and xylazine (7 mg/kg), with supplementary doses administered as required. The study protocols were approved by the VA Loma Linda Healthcare System's Institutional Review Board (IRB) for humans and their Institutional Animal Care and Use Committee (IACUC) for the three laboratory-animal species.

B. DPOAE measures

All experimental methods utilized for humans (Martin *et al.*, 2009), rabbits, chinchillas, and rats (Martin *et al.*, 2010a,b) were highly similar to those described previously. For all subjects, DP-grams as a function of the f_2 frequency were measured in 0.1-oct steps at optimal f_2/f_1 ratios and at various L_1, L_2 levels to establish normal baseline DPOAEs. The equipment used to measure DPOAEs was similar to that described recently (Martin *et al.*, 2009, 2010a,b). For all species besides the rat, this equipment consisted of a microcomputer (Apple, Macintosh Quadra 700, Cupertino, CA), a two-channel digital-signal processing (DSP) board (Digidesign, Audiomedia, Palo Alto CA), two ear-speakers (Etymotic Research, ER-2, Elk Grove Village, IL), and a low-noise microphone assembly (Etymotic Research, ER-10A, Elk Grove Village, IL). In concert, this equipment generated the two primary tones, i.e., f_1 and f_2, and simultaneously measured the level of the ear-canal sound pressure. For

DP-grams, the ear-canal signal was synchronously sampled at 44 100 Hz and averaged (humans $n=8$; laboratory species $n=4$) to obtain a 4096-point sample. From a fast-Fourier transform (FFT) of the time sample, the $2f_1-f_2$ and $2f_2-f_1$ DPOAEs and associated noise-floor (NF) levels were measured. The NF was based upon the average of $n=8$ frequency bins on either side of the DPOAE-frequency bin, excluding the first bin on either side of the DPOAE frequency.

In the rat, a dynamic signal analyzer board (NI PCI-4461, National Instruments, Austin, TX) was used with the sampling rate set to 176 400 Hz for a 16 384-point sample to measure DP-grams. The NF in this case was based on the average of $n=12$ bins on either side of the DPOAE-frequency bin, excluding the first six bins on either side of this bin. All other equipment for rats was as described above for the other species, except that an Etymotic ER-10B+ microphone system was used instead of the ER-10A.

C. DPOAE level/phase (L/P) maps

DPOAE L/P maps formed the primary basis for comparing DPOAEs between the four species. These maps were created by measuring DPOAEs in response to constant-ratio sweeps where f_2/f_1 was varied from 1.025 to 1.5, in 0.025 increments. The L/P maps can be thought of as a collection of DP-grams arranged so that DPOAE frequency steps of ~44 Hz can be plotted along the abscissa. For all species, DPOAEs were measured from 0.5 to 6 kHz, with f_1 ranging from 0.258 to 12.016 kHz, and f_2 from 0.366 to 18.023 kHz. DPOAE L/P maps were based upon an FFT of an averaged 2048-point time sample for all species except the rat, which as noted above, was the same as that used to obtain DP-grams. DPOAE level was then directly plotted (Microsoft Excel 2003, v.11.5, Redmond, WA), while phase, before plotting, was corrected for primary-tone phase variation and unwrapped by "looking" in two directions (ratio and frequency) using custom-developed spreadsheet routines. Final plots were constructed using technical-computing software (MathWorks, MATLAB, v.R2010A, Natick, MA). The resulting DPOAE L/P maps were highly similar to those described by Knight and Kemp (2000, 2001) in which DPOAE magnitude and phase were plotted as a function of the f_2/f_1 ratio and DPOAE frequency. The primary-tone levels were chosen to be just intense enough to produce robust emissions throughout the L/P map for each species. Thus, in humans, these maps were obtained with $L_1=L_2=75$ dB SPL, while in the other species $L_1=L_2=65$ dB SPL was used.

DPOAE L/P maps were produced with and without (control) an IT placed either at 44 Hz below the DPOAE frequency, or with an IT placed at one-third of an octave above f_2 (i.e., 1/3-oct IT). The IT was digitally mixed with f_1 and the two-component signal presented on the f_1 channel. The IT was also rotated in phase by 90° after each sample in order to cancel the majority of emission components produced by the addition of a third tone in the final average, which was composed of either four or eight samples (see Fahey *et al.*, 2000). The ITs were presented on alternate trials to minimize any effects due to either cochlear efferent activity or time-dependent changes in the measured DPOAEs. In humans, the IT near f_{dp} was set to 65 dB SPL and the 1/3-oct IT was presented at either 75 or 80 dB SPL. In the three laboratory species, the IT near f_{dp} was set to 55 dB SPL and the 1/3-oct IT was presented at 75 dB SPL. To reveal the effects of the IT, vector differences were computed between control DPOAE L/P maps and those obtained in the presence of the IT to produce residual DPOAE L/P maps. The magnitude and phase of the DPOAE L/P maps in the presence of the IT, and the resulting residual maps were plotted identically to the control maps.

DP-grams with and without the IT and the resulting residual were extracted from the DPOAE L/P maps for humans ($f_2/f_1=1.2$) and for the other species ($f_2/f_1=1.25$) near their optimal primary-tone ratios. So that the DP-grams could be easily compared to the DPOAE L/P maps they were plotted as a function of DPOAE frequency rather than the more typical f_2 frequency. The phase of the residual was unwrapped in the frequency direction and described as a function of DPOAE frequency and phase in cycles. Plotted in this manner, the slope is in units of time and thus can be thought of as a delay in milliseconds.

III. RESULTS

The results presented below first illustrate for each of the four species the DP-grams and residuals extracted from the DPOAE L/P maps at their optimal f_2/f_1 ratio. The DP-grams with and without an IT placed near the f_{dp} (panel A1) or for a 1/3-oct IT (i.e., the IT placed 1/3 octave above f_2—panel A2) are equivalent to those that can be obtained by the more traditional DP-gram methods. The A3 plot near the top right of each figure compares the resulting phase gradients of the residuals obtained for each of the DPOAE-level results illustrated in panels A1 and A2. In the B and C panels below, these findings are expanded across a broad range of f_2/f_1 ratios by presenting a series of DPOAE L/P maps. The legends at the top right describe the DPOAE magnitudes and phases. In general, the darker shading of the top legend represents the lower-level emissions, while the lighter shading depicts mid to higher level DPOAEs. The DPOAE phase legend below is partitioned into 45° sections, with phase advancing in a counterclockwise direction. While the print versions of the figures are in various shades of black and gray, their online counterparts are in color.

A. DPOAE components in humans: DP-grams at optimal ratios and DPOAE L/P maps

Panel A at the top of Fig. 1 presenting measures from the right ear of the representative human subject HV9-R demonstrates the ability to extract DPOAE components from both near the f_{dp} as well as DPOAE constituents presumably arising basal to a 1/3-oct IT. The first plot in Fig. 1-A1 at left shows DP-grams and residuals extracted by an IT near the f_{dp}, while a similar plot is shown in panel Fig. 1-A2 for the outcome of introducing a 1/3-oct IT. A third plot in A3 compares the resulting phase gradients of the residuals obtained for each of the DPOAE-level results illustrated in panels A1 and A2. Note that the phase line style matches with that of its amplitude residual counterpart in Figs. 1-A1 and 1-A2. A

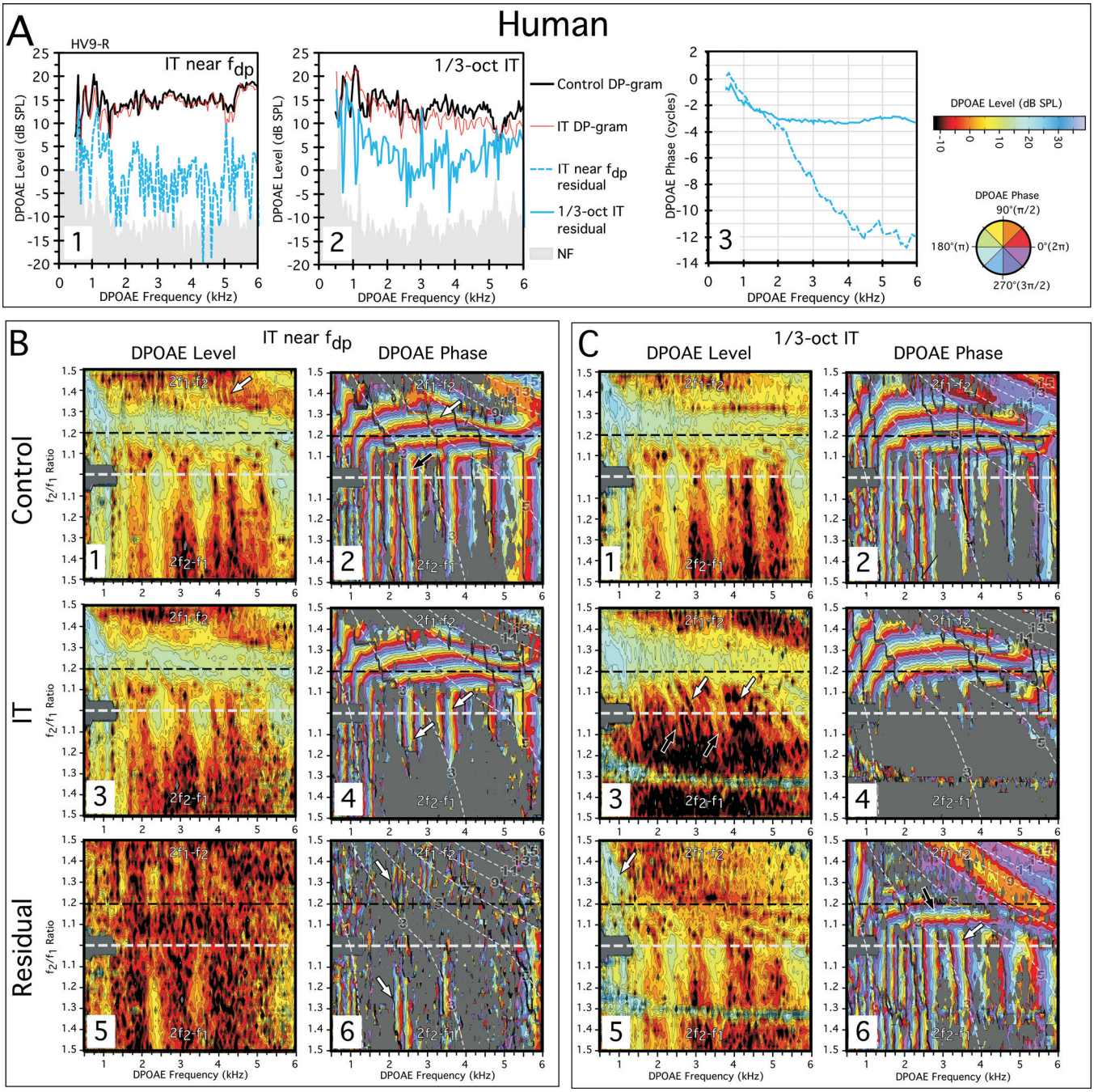

FIG. 1. (Color online) (A) DP-grams and (B, C) DPOAE L/P maps for a normal human measured at L_1, $L_2 = 75$, 75 dB SPL. DP-grams in A1 obtained with an IT near f_{dp} (light gray line at top) or without an IT (black line) demonstrate the ability in humans to extract a residual with a steep phase gradient (dashed gray line in A3) consistent with a DPOAE reflection component from f_{dp} (dashed gray line at bottom in A1). DP-grams in A2 show that an even larger residual (gray line at bottom) with shallow phase slope (light gray line in A3) indicative of a distortion component can be obtained with a 1/3-oct IT. Panel B shows DPOAE L/P maps with the IT near f_{dp}. The IT removes some, but not all of the vertical phase banding (white arrows in B4) and extracts a small patchy residual (B5) with vertical phase banding (white arrows in B6). Panel C shows the effects of a 1/3-oct IT on DPOAE L/P maps. Here the IT removes essentially all the vertical phase banding (C4) and extracts a residual (C5) with both horizontal (black arrow in C6) and vertical phase bandings (white arrow in C6) suggesting that DPOAE components with both reflection- and distortion-like properties arise basal to the IT in humans. On this and subsequent figures, the black dashed horizontal lines on the level and phase plots demark the optimal f_2/f_1 ratio for acquiring commonly measured $2f_1-f_2$ DP-grams. On all DPOAE L/P maps, data for the $2f_1-f_2$ and $2f_2-f_1$ DPOAEs are displayed above and below, respectively, the white dashed horizontal line at $f_2/f_1 = 1.0$ (not labeled). The thin white diagonal dashed lines through the phase plots (panels B and C−2, −4, −6) represent constant f_2 trajectories beginning at 15 kHz in the top right of each plot, and ending at 1 kHz in the lower left region that can be used as a reference for this and other DPOAE L/P maps. See text for complete details of this and following figures.

standard control DP-gram (i.e., no IT present) is represented in Fig 1-A1 by the solid black line at the top of the plot. This particular DP-gram appears to demonstrate DPOAE fine structure as evidenced by the presence of a series of peaks and valleys, especially around 0.5 to about 2 kHz. The thin gray line intertwining with this control measure shows the DP-gram obtained on alternate trials in the presence of a 65-dB SPL IT near the f_{dp}. For this specific subject, the DP-grams with and without the IT were very similar, except for a limited amount of the often-observed reduction in fine

structure when an IT is near the f_{dp}. Interestingly, some of the largest peaks and valleys in the DP-gram between ~0.5 and 1.5 kHz were relatively unaffected by the 65-dB SPL IT in this ear. The vector difference between these two conditions (i.e., control vs IT) yielded a small residual (dashed gray line) just above the NF (shaded gray region). In the adjacent A2 plot, identical data are shown, but this time the 1/3-oct IT protocol was utilized. Again, the control (solid black line) and the 1/3-oct IT (thin gray line) DP-grams were quite similar. However, the 1/3-oct IT DP-gram was consistently a few decibels lower in magnitude, except at the lowest test frequencies. In addition, the DPOAE fine structure seemed relatively unchanged apart from the aforementioned low-frequency region, where some of the largest peaks and valleys were diminished. The 1/3-oct IT produced a much larger residual (thick gray line) when the vector difference was computed, particularly in the low-frequency region where this component likely played a role in producing the large peaks and valleys observed for the control DP-gram condition. This residual presumably represented basal DPOAE components that were removed by the IT.

The plot at the far right in panel A3 displays the phase of the DPOAE components revealed by the IT near the f_{dp} (sloping dashed gray line) along with those extracted by the 1/3-oct IT (horizontal solid gray line). It can be seen from these data that the DPOAE residual extracted by an IT near the f_{dp} exhibited a steep phase slope indicative of a reflection-based DPOAE component. Conversely, the DPOAE constituent revealed by the 1/3-oct IT demonstrated a shallow slope that was thought to be the signature of DPOAEs generated near the peak of the f_2 TW, i.e., a distortion component. However, these latter DPOAE constituents appeared to originate at, or basal to, the IT-frequency place at 1/3 octave or more above f_2. For the 1/3-oct IT condition, the residual phase gradients were steeper for the DPOAE frequencies below about 2 kHz. This outcome corresponds to a bending over of the phase bands that can be appreciated in the DPOAE L/P maps described below (e.g., see B2, C2). This curvature presumably occurred because of the collapse in cochlear scaling at the very apex of the cochlea. Overall, these data revealed the predicted source of DPOAEs reflected from f_{dp} in humans, and add to the two-source formulation the possibility of additional DPOAE components generated basal to f_2 in the tails of the primary-tone TWs.

The above evidence for substantial basal DPOAE components is reinforced in much more detail in the human DPOAE L/P maps described below where DPOAEs were measured over a wide range of f_2/f_1 ratios, and with DPOAE frequencies ranging from 0.5 to 6.0 kHz. The plots in Fig. 1(B) represent the experiment in which the IT was presented near the f_{dp}, while those in Fig. 1(C) illustrate the outcomes when the 1/3-oct IT was utilized. In both Figs. 1(B) and 1(C), the control DPOAE L/P maps without ITs are presented in the top row, while similar plots with ITs present are displayed in the middle row. The plots in the bottom row of these two panels illustrate the residual DPOAE L/P maps, which are based upon the vector differences between the control and either one of the IT conditions. Each DPOAE-level map illustrated in the left columns of Figs. 1(B) and 1(C) is accompanied by a map of the corresponding DPOAE phase in the adjacent right columns.

In the control condition depicted in Fig. 1-B1, robust DPOAEs were obtained for subject HV9-R that were maximal around the optimal f_2/f_1 ratio of 1.2 (dashed black line). For the corresponding control phase map shown in panel B2, both horizontal (white arrow at ~f_2/f_1 ratios of 1.3) and vertical phase banding were observed with vertical banding predominately below f_2/f_1 ratios of about 1.1 (black arrow). In the "IT near the f_{dp}" condition depicted in panel B3, the faint vertical striations that were visible in the control map of panel B1 (white arrow at top ~4 kHz), which likely represent fine-structure interference from reflection components, were smoothed out and no longer apparent. Additionally, a few other level changes were observed consisting of mainly a reduction in the wide-ratio $2f_2-f_1$ DPOAE levels. In the matching phase map of panel B4, the IT near f_{dp} removed some of the vertical phase banding for the $2f_1-f_2$ and $2f_2-f_1$ DPOAEs, but distinct vertical phase bands remained for both emissions (white arrows). In the residual condition shown in panel B5, a very small $2f_1-f_2$ DPOAE residual (light grays) was extracted that was just barely above the NF (pure black). When examined closely, it is obvious that this residual emission exhibited very narrow vertical phase bands (white arrows) in B6, as would be expected for a reflection DPOAE, which is consistent with the steep phase gradient obtained for this component at the optimal ratio (see corresponding dashed line in A3).

In Fig. 1(C), the effects of a 1/3-oct IT on the DPOAE L/P maps of the same subject HV9-R are shown. By comparing the IT level maps of panels C1 vs C3, it is clear that the 1/3-oct IT removed most of the narrow-ratio $2f_1-f_2$ DPOAEs (white arrows in C3) and essentially all of the $2f_2-f_1$ DPOAE (black arrows below). In the corresponding 1/3-oct IT phase plot of panel C4, it is evident that essentially all of the vertical phase banding was eliminated by the IT in this condition, thus, suggesting that in humans, DPOAEs with reflection-like phase characteristics can arise basal to the 1/3-oct IT, while only a small DPOAE component is actually reflected from the f_{dp}. A substantial residual was revealed in the level map of panel C5 for this condition. The residual was largest for the $2f_1-f_2$ DPOAE at f_2/f_1 ratios $\lesssim$1.2, except for low frequencies ($f_{dp}\lesssim$1.5 kHz) where it was large at all ratios (white arrow). From inspection of panel C6, it is apparent that for the $2f_1-f_2$ DPOAE components with both reflection (white arrow) and distortion (black arrow above) phase properties were extracted, while the $2f_2-f_1$ emission uniformly exhibited vertical reflection-like phase banding. The residual for narrow-ratio $2f_1-f_2$ DPOAEs and for all $2f_2-f_1$ DPOAEs was very similar with respect to size and phase characteristics to the control "no IT" condition thus implying that these emissions are composed largely of basal sources.

B. DPOAE components in laboratory species: DP-grams at optimal ratios and DPOAE L/P maps

For comparison purposes, DPOAE L/P maps were measured and DP-grams extracted from these maps in rabbits, chinchillas, and rats under as nearly identical conditions

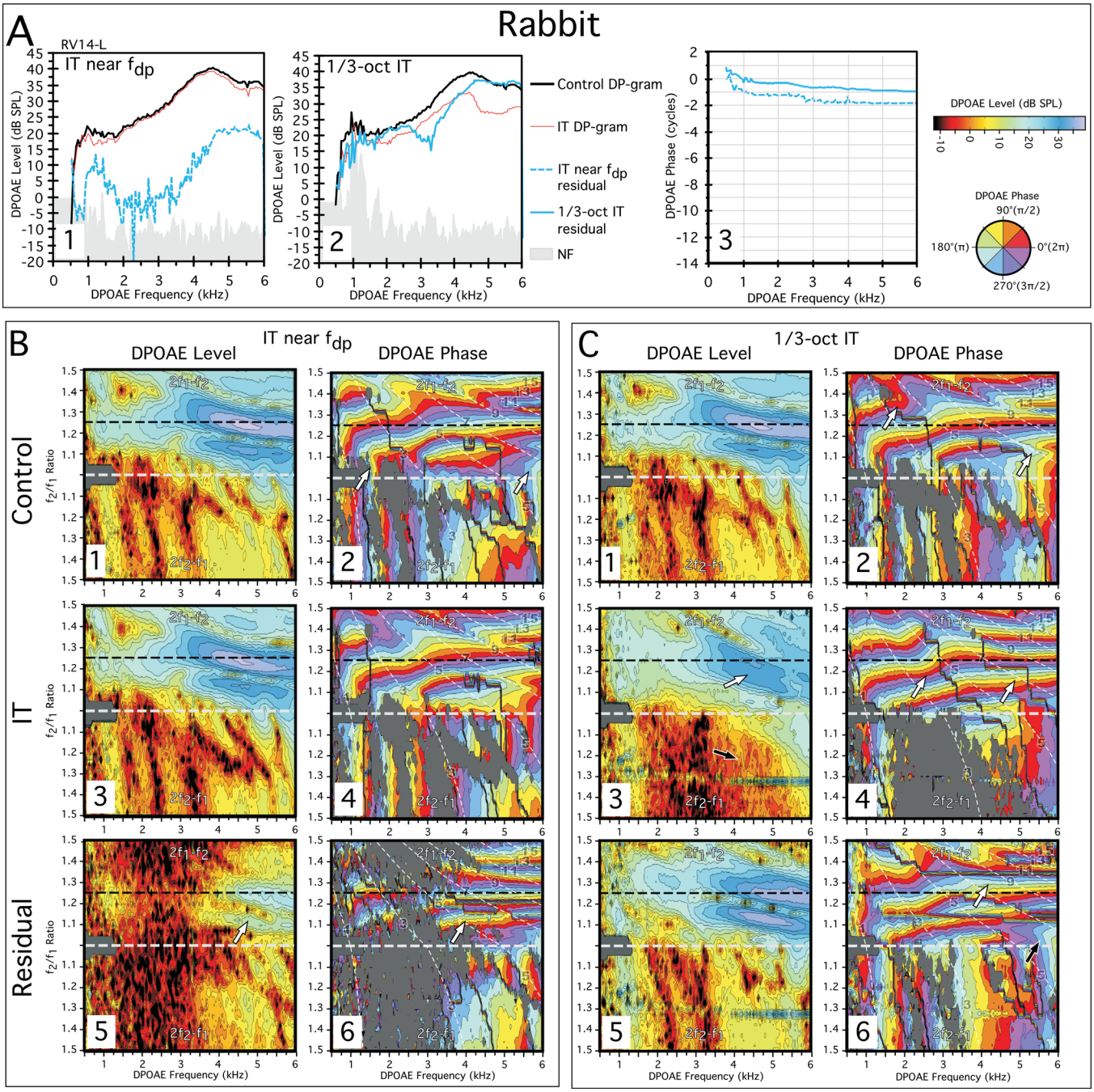

FIG. 2. (Color online) (A) DP-grams and (B, C) DPOAE L/P maps for a rabbit illustrating the effects of an IT near f_{dp} or a 1/3-oct IT. In the rabbit DP-gram analysis, both IT conditions were capable of extracting residuals but they were associated with shallow phase slopes (A3) consistent with a DPOAE distortion component. The DPOAE L/P maps with the IT near f_{dp} (B) and with the 1/3-oct IT (C) supported and extended the DP-gram findings. Thus the near f_{dp} IT had little effect on the DPOAE L/P maps, but did extract a small residual (white arrow in B5) with clear horizontal phase bands indicative of a distortion component (white arrow in B6). In the 1/3-oct IT situation, the IT removed essentially all the vertical phase banding obvious in the control (C2) L/P plot, and the DPOAEs were associated with very orderly horizontal phase bands (white arrows in C4). The residual was large (C5) and contained both horizontal (white arrow in C6) and vertical banding (black arrow in C6) consistent with the existence of both reflection- and distortion-like components at or above the 1/3-oct IT-frequency place.

as possible to those described above for human subjects. The gray scales on the level maps are the same as those shown above for humans, so that the differences in DPOAE levels can be compared across species. Since all DP-grams and DPOAE L/P maps have the same basic format, only the most salient features are described for the three laboratory species.

Figure 2 shows DP-grams and DPOAE L/P maps measured from the left ear of a representative rabbit (RV14-L) with normal cochlear function. In the A panels, DP-grams at the optimal f_2/f_1 ratio of 1.25 are illustrated for both an IT near the f_{dp} (A1) and a 1/3-oct IT (A2). Note in panel A1, the relative lack of fine structure in the rabbit control DP-gram (black line), which evidences DPOAE levels that are much larger as compared to those displayed by the human DP-gram (see black line in Fig. 1-A1). When the IT was placed near the f_{dp}, a small residual (dashed gray line in lower portion of A1) could be extracted at low frequencies,

along with a considerably larger one at frequencies above 4 kHz. However, unlike that in humans, this residual exhibited a shallow phase gradient (dashed gray line in A3) indicative of a distortion component. The 1/3-oct IT condition revealed a very large residual component (thick gray line) illustrated in A2 that also exhibited a shallow phase slope shown by the solid gray line in A3. As described above for humans, a steeper phase gradient was once more observed for DPOAE frequencies below ~1 kHz, which again corresponds to the curvature in the phase banding observed below in the control phase maps of Figs. 2-B2 and 2-C2 at similar frequencies. Thus, at optimal f_2/f_1 ratios, rabbits did not display significant reflection components based upon phase characteristics that can be extracted by placing an IT near the f_{dp}. However, they did exhibit a large DPOAE component with a shallow phase slope that presumably arose basal to the 1/3-oct IT, much like that observed for humans.

Figure 2(B) presents DPOAE L/P maps obtained with and without an IT near the f_{dp}, while the plots in Fig. 2(C) illustrate similar measures for the with and without 1/3-oct IT conditions. Again, it can be noted from inspection of the control no-IT DPOAE level map of panel B1 that rabbits have much larger DPOAEs than humans in that their emissions can approach 40 dB SPL at optimal ratios (dashed black line) as shown here. In this particular rabbit, in the corresponding control phase map of panel B2, small regions of vertical phase banding were present at f_2/f_1 ratios <1.1 near DPOAE frequencies of 1.5 and 5.5 kHz (white arrows). When the IT was placed near the f_{dp} as shown in the corresponding level and phase maps of panels B3 and B4, respectively, only small effects were evident. The comparable residuals revealed by the IT near the f_{dp} and illustrated in panels B5 and B6 were confined primarily to DPOAE frequencies >4 kHz (white arrows). In agreement with the findings displayed above in A3, mostly horizontal phase banding was observed for this residual (white arrow in B6), which is consistent for a distortion component with a shallow phase gradient.

For the interference condition of Fig. 2(C) in which the IT was placed 1/3-oct above f_2, the results were dramatically different. As shown in panel C3, the 1/3-oct IT significantly reduced the overall level of the $2f_1-f_2$ DPOAEs (white arrow), and abolished many of the $2f_2-f_1$ DPOAEs, especially at higher f_2/f_1 ratios (black arrow), as compared to the control condition illustrated in panel C1. It also eliminated a prominent horizontal notch near an f_2/f_1 of 1.2 in the $2f_1-f_2$ DPOAE levels and many of the phase irregularities evident in the control phase map of panel C2 (white arrows). This resulted in more uniform and slightly narrower horizontal phase bands in panel C4 (white arrows). Such observations are consistent with the suggestion that the 1/3-oct IT removed DPOAE components that were normally mixing in the control condition. The residual revealed by vector subtraction of the IT condition and displayed in panel C5 was large thus accounting for the reduction in DPOAE levels in the IT condition of panel C3. The phase behavior of this residual shown in panel C6 exhibited both horizontal (white arrow) and vertical phase bands (black arrow), much like the control condition illustrated in C2. Overall, in the rabbit, the IT near the f_{dp} had little effect on the DPOAE L/P maps, particularly for the $2f_1-f_2$ emission, while a 1/3-oct IT removed large DPOAE components with both reflection-like and distortion phase properties. With respect to the 1/3-oct IT condition, the rabbit showed effects that were similar to those observed for human subjects. The major difference between the two species was the lack of any measurable reflection components arising from the f_{dp} in the rabbit.

Figure 3 shows data from similar experiments for the right ear of a representative chinchilla (CV4-R). The standard DP-gram analysis (black line) displayed in Fig. 3-A1 shows a highly repeatable and notable feature of the chinchilla DP-gram, i.e., several prominent notches from ~1.5 to 3 kHz. These notches were unaffected by the presentation of an IT near the f_{dp} (thin gray line). The vector difference between these two conditions produced a small residual (dashed gray line below). The phase slope of this residual above 3 kHz shown in panel A3 was shallow (dashed gray line), similar to that observed in the rabbit (see Fig. 2-A3). When DP-grams were obtained with a 1/3-oct IT, as evident in panel A2, the prominent notch around 1.5 kHz was significantly reduced and overall the IT DP-gram (thin gray line) was smaller in level than the control DP-gram. In contrast to the near f_{dp} situation, a very large residual (thick gray line) shown in A2 was revealed that demonstrated a predominately shallow slope (solid gray line of panel A3) that was not markedly different from the component extracted by the IT placed near the f_{dp}. In both cases, these phase characteristics were consistent with a distortion component. At frequencies below about 2 kHz, a steeper phase slope was again evident for this region that corresponded to the pronounced apical phase curvature in the control DPOAE phase maps of Figs. 3-B2 and 3-C2. Such findings were similar to those described above for both humans and rabbits. It appears, then, that at optimal f_2/f_1 ratios, any DPOAE components that can be extracted in chinchillas exhibit phase gradients which are consistent with distortion rather than reflection-based mechanisms.

Figure 3(B) shows DPOAE L/P maps for the IT near the f_{dp} condition. From scrutiny of the control DPOAE-level map of B1, it is clear that this chinchilla displayed very large DPOAEs for both the $2f_1-f_2$ and $2f_2-f_1$ emissions. When present, the $2f_2-f_1$ DPOAE was considerably larger than observed in the rabbit (see Fig. 2-B1). The notches observed for the optimal ratio DP-grams were also apparent running along a diagonal through the control-level map (white arrows) of panel B1. In the related control phase map of panel B2, both vertical and horizontal phase banding was again evident, with prominent vertical bands originating near f_2/f_1 ratios <1.1 for the $2f_1-f_2$ DPOAE that were contiguous with the vertical banding that corresponded to the $2f_2-f_1$ DPOAE (white arrows). As seen previously for the rabbit, the IT near the f_{dp} produced little change in either the level (B3) or phase (B4) of the DPOAE L/P maps as compared to the control condition. However, as illustrated in panel B5, the IT did extract a much larger residual than observed above for the rabbit throughout most of the level-map area. The phase properties of this residual shown in panel B6 were a complex mixture of horizontal (white

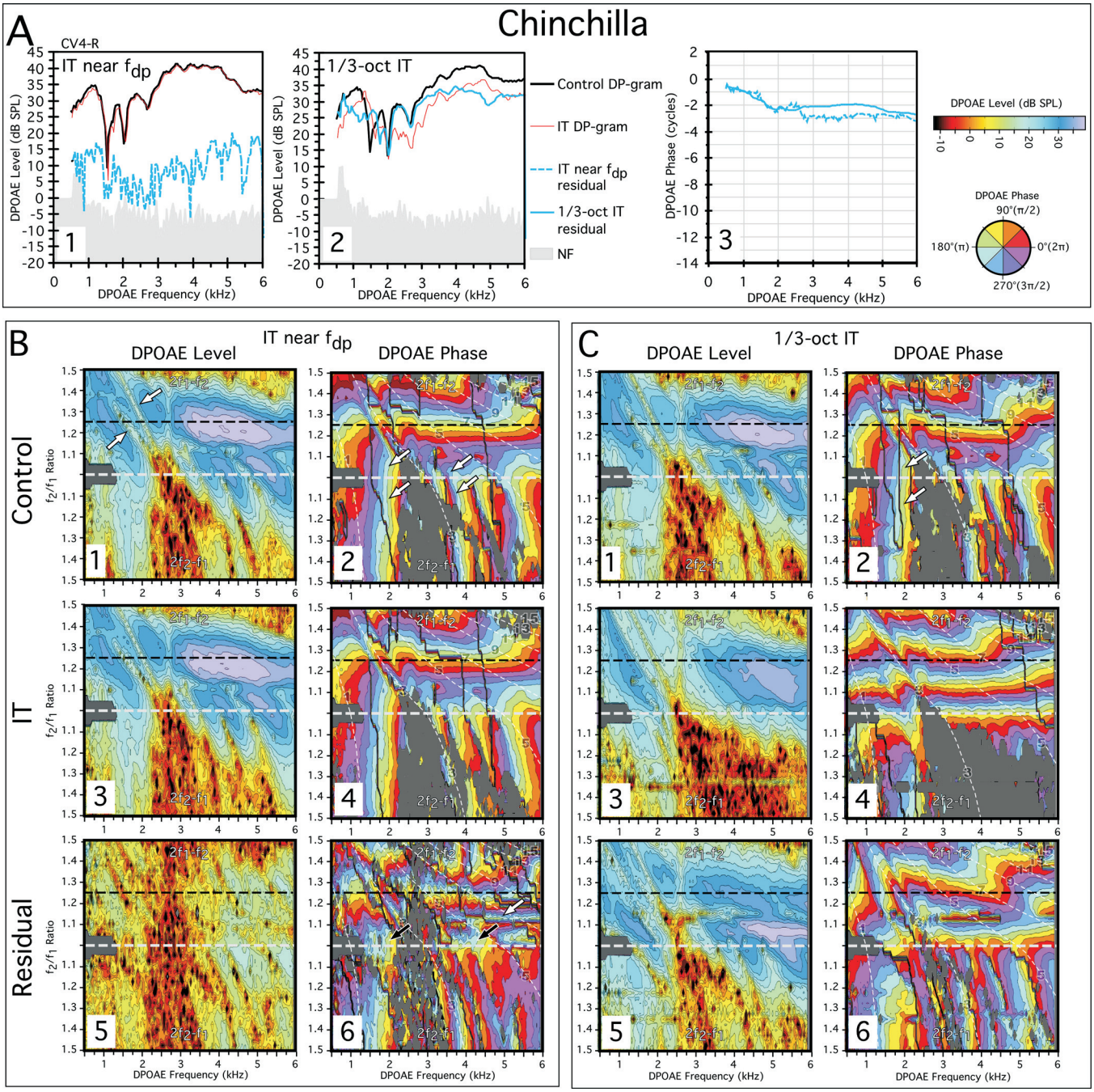

FIG. 3. (Color online) (A) DP-grams for a chinchilla and (B) corresponding DPOAE L/P maps illustrating the effects of an IT near f_{dp} or (C) a 1/3-oct IT. In the DP-grams, regardless of the location of the IT, residuals exhibited shallow phase slopes (A3) except for a small segment associated with apical curvature observable in the DPOAE L/P maps of all species. The IT near the f_{dp} extracted a larger residual (B5) than in the rabbit, with a mixture of phase patterns (B6), with some being clearly horizontal (white arrow in B6), and others being somewhat vertical (black arrows in B6) making it difficult to rule out the existence of reflection components in the chinchilla. In the 1/3-oct IT condition, the IT removed essentially all vertical phase banding (C4) leaving behind a phase map with very orderly horizontal-phase characteristics. The residual extracted by the 1/3-oct IT was very large (C5), and contained both horizontal and vertical bandings again consistent with the existence of both reflection- and distortion-like components at or above the 1/3-oct IT frequency place.

arrow) and poorly defined vertical phase bands (black arrows), unlike the rabbit, in which a small residual was clearly dominated by horizontal phase banding. Thus, in the chinchilla, the existence of some small DPOAE components reflected from the f_{dp} could not be ruled out.

For the 1/3-oct IT condition depicted in the plots of Fig. 3(C), a familiar pattern was observed that was similar to the rabbit findings. Thus, in the IT condition, the complicated phase structure observed for the control condition in C2 was turned into a very orderly horizontal phase pattern presented in panel C4. Particularly striking in C4 was the removal of a very prominent region of vertical phase banding for the $2f_1-f_2$ and $2f_2-f_1$ DPOAEs over the low frequencies from ~0.5 to 2 kHz, as well as essentially all the vertical phase bands above the notch from ~3.5 kHz to the high-frequency end of the map. Presumably, these DPOAE components with

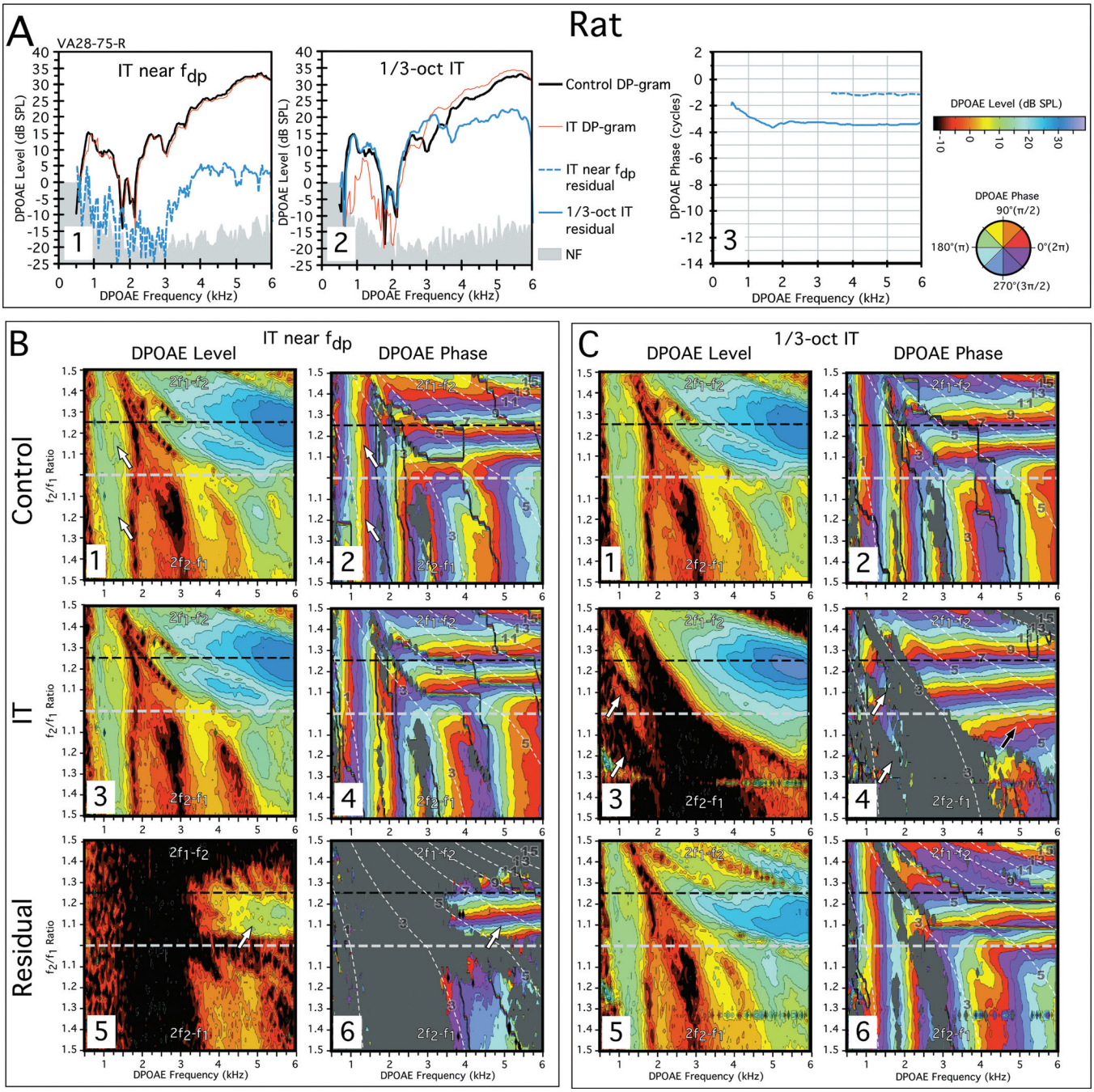

FIG. 4. (Color online) (A) DP-grams and (B) DPOAE L/P maps for a rat showing the effects of an IT near f_{dp} or (C) a 1/3-oct IT. The near f_{dp} IT DP-gram analysis for the rat revealed a small high-frequency residual (dashed gray line in A1) with a shallow phase slope (dashed gray line in A3). A much larger residual was revealed by the 1/3-oct IT (A2) with similar phase characteristics (solid gray line in A3). In the rat the DPOAE L/P maps were characterized by a large low-frequency component (white arrows in B1) with very striking vertical phase banding (white arrows in B2) for both $2f_1-f_2$ and $2f_2-f_1$ DPOAEs. Regardless of the reflection-like phase properties of this component, the IT near f_{dp} had essentially no effect on the level (B3) or phase (B4) of this or other regions of the maps for the IT condition in spite of prominent vertical phase banding in the other DPOAEs above this low-frequency region. The small residual that could be extracted (white arrow in B5) was dominated by horizontal phase bands (B6). In the 1/3-oct IT condition, the most remarkable feature was the ability of the IT to almost completely remove the low-frequency component for both the $2f_1-f_2$ and $2f_2-f_1$ DPOAEs (region of white arrows in C4) and all the associated vertical phase banding (region of white arrows in C3) observed for the control condition of C2 leaving the resulting phase map (C4) dominated by nearly perfect horizontal phase bands. Thus, a very large portion of the rat DPOAE space was apparently composed of DPOAEs arising basal to the 1/3-oct IT place on the BM.

reflection-like phase banding originated from regions basal to the 1/3-oct IT. Further, a large residual was revealed by vector subtraction of the IT condition in C5 with a phase pattern in C6 that was very similar to that of the control condition shown in panel C2. Overall, in the chinchilla, the type of DPOAE components extracted by the IT near the f_{dp} were difficult to interpret with evidence for a distortion component possibly accompanied by a smaller reflection constituent. The findings for the 1/3-oct IT were similar to those observed for the human and rabbit in that a large DPOAE residual was extracted. This residual for the $2f_1-f_2$ DPOAE exhibited primarily distortion-like horizontal phase banding

that was distorted by the notches, while the $2f_2-f_1$ residual was dominated by reflection-like vertical phase banding, which is typical for this emission.

A final data set is presented in Fig. 4 for the right ear of a representative rat subject (VA28-75-R). In Fig. 4-A1, DP-grams are shown for an IT near the f_{dp} and in panel A2 for a 1/3-oct IT. It is clear for the f_{dp} IT situation of panel A1 that both DP-grams without (black line) and with the IT (thin gray line) were essentially superimposed, and a residual (dashed gray line) could only be measured at DPOAE frequencies >3 kHz. In addition, the IT had little effect on a prominent notch in the rat DP-gram that can be seen as a major feature in the DPOAE L/P maps described below. The slope of the residual from the near the f_{dp} condition shown in A3 (dashed gray line) was shallow, and thus consistent with a distortion component. In the 1/3-oct IT case illustrated in A2, a large residual (thick gray line) was obtained at all DPOAE frequencies, which represented a finding that was similar to that described above for humans, rabbits, and chinchillas. In panel A3, this residual also exhibited a two-part slope with the initial segment for DPOAEs <2 kHz being steeper than the final segment that was very shallow. However, unlike that of the other species, this steep portion corresponded to a unique region of DPOAEs below ~1.8 kHz that was accompanied by almost perfectly vertical phase bands seen below in the control DPOAE phase maps of B2 and C2 that extended across all f_2/f_1 ratios for both emissions. Thus, this component had reflection-like properties, which clearly originated not from the f_{dp}, but at or above the 1/3-oct IT frequency place. The remaining residual above this region had a shallow phase slope consistent with a distortion component.

Figure 4(B) illustrates DPOAE L/P maps obtained with an IT near the f_{dp}. In the control-level map of B1, the notch observed in the DP-grams of panel A was obvious throughout the map. As previously mentioned, an unusual feature of this map was a large region of DPOAEs below ~1.8 kHz for both $2f_1-f_2$ and $2f_2-f_1$ DPOAEs (white arrows in B1) that exhibited almost perfect vertical phase banding across both $2f_1-f_2$ and $2f_2-f_1$ emissions (white arrows in B2). As in the other laboratory species, for DPOAE L/P maps with the IT near the f_{dp}, there was little apparent difference, if any, between the control and IT conditions with respect to either the level (B1 vs B3) or phase maps (B2 vs B4). In the residual-level map for this rat shown in panel B5, a relatively large component was apparent above DPOAE frequencies of ~3.5 kHz (white arrow) that very clearly displayed horizontal phase banding (white arrow) in the corresponding phase map of panel B6 and not the expected vertical phase banding that would be present, if it were reflected from the f_{dp}.

Figure 4(C) displays results for the 1/3-oct IT condition. Here, the 1/3-oct IT removed a large region of $2f_1-f_2$ and $2f_2-f_1$ emissions as shown in panel C3 (white arrows) and all the vertical phase banding (white arrows in C4), for the low-frequency DPOAEs as well as for all DPOAEs above this region. The remaining DPOAEs were associated with very orderly horizontal phase characteristics as shown in panel C4 as compared to the control condition of panel C2. For the $2f_2-f_1$ DPOAEs an unusually large region of emissions with horizontal-like phase banding remained (black arrow in C4). In addition, a large DPOAE residual was apparent in the level map of panel C5, which was associated with a phase pattern shown in C6 that was highly similar to that observed for the control no-IT condition of panel C2. Thus, for the rat, the 1/3-oct IT yet again seemingly removed basal DPOAE components with both distortion- and reflection-like characteristics that originated basal to the IT-frequency place.

IV. DISCUSSION

The present study was designed to compare DPOAE components that could be extracted by ITs placed near f_{dp} or at 1/3-oct above f_2 (i.e., 1/3-oct IT) in humans as compared to three laboratory-animal species. In humans, for the $2f_1-f_2$ DPOAE, a small reflection component was extracted by the IT near f_{dp}, and this component was characterized by a steep phase slope as would be expected from a reflection-based mechanism. However, vertical phase banding remained that could not be removed by the IT (see Fig. 1-B4). Thus, the present methods were capable of revealing a reflection component in humans predicted by the two-source model of DPOAEs (e.g., Shera and Guinan, 1999). However, this component was difficult to extract in the DP-gram analyses and it was barely detectable in the DPOAE L/P maps based upon the limited amount of time averaging ($n=8$). In fact in the DPOAE L/P maps, only three of the ten normal-hearing subjects had detectable reflection components. This observation is not surprising considering that in a recent study by Abdala and Dhar (2010) the average level of the reflection component was at the best –3 dB SPL and in most cases averaged between –10 and –15 dB SPL. It should be emphasized that in the present example (e.g., Fig. 1), removal of the reflection component did decrease fine structure as described by others. On the other hand, most DPOAE fine structure did not appear to be affected by the reduction of basal DPOAE components by the 1/3-oct IT except for at the lowest frequencies. The residual at optimal ratios (black arrow in Fig. 1-C6) is consistent with this observation and indicates that basal components have shallow phases similar to that of the f_2 components and thus the basal components would tend to add at a fairly constant phases difference which would not produce significant fine structure except at low frequencies where the phase gradient becomes steeper.

Essentially identical methods to those utilized in humans were applied to the three laboratory species, namely, the rabbit, chinchilla, and rat. However, these experiments failed to provide any conclusive evidence for reflection components arising from the f_{dp} in any of these species. This is remarkable in that the DPOAEs in all these animals are much larger than those measurable in humans, even at the lower primary-tone levels utilized here. Thus, if the reflection from the DPOAE-frequency locus was significant in these species, then it should be easily detectable or, at least, comparable to those "exceptional" human subjects with robust DPOAEs and prominent fine structure. In fact, the lack of fine structure in the DP-grams of these animals is consistent with the absence of any significant reflection component. It should be emphasized that the present data obtained from these common

laboratory species were obtained with a minimum of averaging ($n=4$), because of the considerable time of nearly an hour required to collect the DPOAE L/P maps with and without an IT. Thus, the present results were not specifically intended to eliminate the possibility that some detectable reflection from f_{dp} occurs in these laboratory species. In fact, in the chinchilla, there was some but certainly not conclusive evidence, for a very small reflection component.

In the rabbit, the IT near the f_{dp} was set to a level at 55 dB SPL that just began to extract a measurable residual for the $L_1=L_2=65$ dB SPL condition in most rabbits. However, at slightly lower levels of the IT, no residual could typically be extracted with ITs near the f_{dp}, even with map regions obtained at twice the frequency resolution and $n=32$ averaging vs the typical $n=4$ time averages (Martin *et al.*, 2010a,b). Consequently, it is reasonably safe to conclude that the DPOAE-reflection components in the laboratory species tested here, if present at all, were minute, i.e., even smaller than those observed in humans.

In rabbit and rat, and somewhat less so in the chinchilla, residual DPOAE phase maps with the IT near f_{dp} revealed components with horizontal phase-banding that was associated with shallow phase slopes in the DP-gram analyses. These represent features, which have previously been attributed to DPOAEs arising from near the peak of the f_2 TW, as opposed to f_{dp} (Shera and Guinan, 1999; Kalluri and Shera, 2001). For distortion components to arise directly from f_{dp} in these species, it would require two inputs into the outer hair cell (OHC) nonlinearity in this region. Based upon the sharp apical cutoff of the primary-tone TWs, any interaction of the primaries at f_{dp} is extremely unlikely. Rather, it seems probable that for certain frequencies the IT suppressed one or both of the primaries in the region of primary-tone overlap, where a significant distortion component is generated, thus revealing this component in the residual. This interpretation is consistent with experiments in rabbits where this distortion-like component could only be detected if the IT was set to a sufficiently high level.

It is important to emphasize that for humans and all three laboratory species, vertical phase banding was present that was relatively unaffected by the IT near f_{dp} for DPOAEs at narrow f_2/f_1 ratios for the $2f_1-f_2$ and at all ratios for $2f_2-f_1$ DPOAEs in the DPOAE L/P maps. Thus by a process of elimination it can be concluded that DPOAEs with these reflection-like characteristics may not originate exclusively from the f_{dp}. An exception to the narrow ratio, reflection-like component for $2f_1-f_2$ was in the rat, which exhibited emissions with vertical phase banding regardless of the f_2/f_1 ratio at low frequencies and for all ratios [see Fig. 4(B)]. This component, too, was unaffected by near f_{dp} ITs thereby inferring that it was not reflected from the f_{dp} place. This component in the rat, as well as at narrow f_2/f_1 ratios in the other species, was contiguous with the $2f_2-f_1$ DPOAE plotted in the lower half of each DPOAE L/P map. The IT near the f_{dp} does have a detectable effect on the $2f_2-f_1$ in all species, however, this effect was small compared to the consequences of the 1/3-oct IT described below.

Overall, it can be stated that all species showed reflection-like DPOAE components associated with vertical phase banding in their DPOAE L/P maps that could not be influenced by ITs near the f_{dp}. In the DP-gram analyses, only in humans a $2f_1-f_2$ DPOAE component could be extracted with the predicted steep phase gradient.

Contrary to what might be expected based upon a two-source model of DPOAEs, in humans the 1/3-oct IT extracted a large residual in the DP-gram analyses, which was associated with a shallow phase slope (see Fig. 1-A3). In the DPOAE L/P maps the 1/3-oct IT eliminated almost all of the narrow-ratio $2f_1-f_2$ DPOAEs, and nearly all of the $2f_2-f_1$ DPOAEs, essentially removing all of the DPOAE components with vertical phase banding in this subject (see Figs. 1-C2 vs 1-C4). The resulting residual was composed of DPOAEs with both reflection- and distortion-like phase characteristics. These results confirmed the outcome described in a previous report in humans (Martin *et al.*, 2009) suggesting that significant DPOAE components in humans are generated at, or basal to, the 1/3-oct IT and that these constituents exhibit both steep and shallow phase characteristics.

In the laboratory-animal species, the effects of the 1/3-oct IT were highly similar in many respects to those described here for humans. For the rabbit, chinchilla, and rat, DP-gram analyses showed that the 1/3-oct IT extracted a residual that was in most cases nearly as large as the DPOAE component measured without the IT. This finding suggests that very large DPOAE components arise at, or basal to, the 1/3-oct IT in these species. This conclusion based upon DP-gram analyses was reinforced by similarly large residuals extracted from the DPOAE L/P maps for the three laboratory species. Such residuals were characterized by having DPOAE components accompanied by both vertical and horizontal phase banding similar to what was observed for humans. A very striking feature in laboratory species was the effect of the 1/3-oct IT on the phase of the remaining DPOAE components in the IT condition. Without exception, the presence of the 1/3-oct IT simplified the complex phase structure observed in the control phase maps resulting in a very organized horizontal phase banding pattern. This effect most likely resulted from the removal of basal DPOAE components, which, in the absence of the 1/3-oct IT, were mixing with the DPOAE elements generated primarily near the f_2 peak region apical to the IT-frequency place. This conclusion appears reasonable, since components near the f_{dp} were undetectable in the laboratory species tested here, and, therefore, this region can be excluded as contributing to the remaining DPOAE components with a very orderly distortion-like behavior.

None of the laboratory species were exactly identical in that they all had features unique to their DPOAE space as revealed by their DPOAE L/P maps. For example, the rabbit had smaller $2f_2-f_1$ DPOAEs than the chinchilla, while both the chinchilla and rat demonstrated large notches in their DP-grams that were visible throughout their DPOAE L/P maps. In addition, the rat provided one of the most unique examples of individual differences where a large region of low-frequency DPOAEs was separated by a large notch throughout the entire DPOAE space [see Fig. 4(C)]. This low-frequency region in the rat was particularly interesting in that the $2f_1-f_2$ DPOAEs, even at wide f_2/f_1 ratios, were dominated by vertical phase banding that was contiguous

with the $2f_2-f_1$ DPOAE. In this case, presentation of the 1/3-oct IT completely eliminated this region of low-frequency DPOAEs that were presumably generated basal to the IT. It should be noted that rat hearing operates over a much higher frequency range than it does in the other species. This circumstance may in some way explain the unusual low-frequency region where DPOAEs appear to be generated almost exclusively basal to f_2 in rats. Humans also have a large DPOAE component at low frequencies and wide f_2/f_1 ratios that also appears to be similarly generated (see white arrow, Fig. 1-C5). Whether or not other common laboratory species such as guinea pigs, gerbils, and mice have basal sources remains unknown. Recently, Martin *et al*. (2010a,b) attributed suppression/enhancement of DPOAEs by ITs presented above f_2 to the existence of basal DPOAE components. Since these phenomena have been observed in guinea pigs and mice (Martin *et al*., 1999) and gerbils (Mills, 1998), it seems reasonable to suggest that these latter species also have substantial basal DPOAE components generated above f_2.

Finally, it should be noted that the 1/3-oct IT removed essentially all the $2f_2-f_1$ DPOAEs in humans and rats, and in significant amounts in the rabbit and chinchilla. These findings are consistent with prior studies (Martin *et al*., 1987, 1998) demonstrating that the $2f_2-f_1$ DPOAE is generated at, or above, its frequency place on the BM.

The present results reinforce the findings of previous studies (Martin *et al*., 2009, 2010a,b) and provide evidence for the existence of basal DPOAE components in two other species. In contrast to the inability to extract a reflection component from the laboratory species as compared to humans, features of these basal DPOAE components were remarkably consistent across all four species. A previous study in rabbits (Martin *et al*., 2010a,b) relied upon the conclusion that DPOAEs "filled in" regions of damage that could subsequently be removed by the 1/3-oct IT as a control for catalyst or other mechanisms masquerading as basal DPOAE components. In the present study, findings in normal rat ears can serve a similar purpose. In the catalyst hypothesis (see Fahey *et al*., 2000), the third tone (IT) creates DPOAEs that appear to be basal sources. However, it seems highly improbable that in the rat these emission components presumably created by the presence of the IT could be of exactly the correct magnitude and phase to completely eliminate both the low-frequency $2f_1-f_2$ and $2f_2-f_1$ DPOAEs, as well as eliminate emissions in other cochlear regions as well (see Fig. 4-C1 and 4-C2 vs 4-C3 and 4C-4). A similar argument would seem to apply, if it was assumed that the IT was simply altering the phase of the f_2 distortion component to produce the large residuals observed. Another weakness of these alternative explanations for apparent basal DPOAE components is that they cannot explain the effects of the 1/3-oct IT on phase behavior, where a disorganized pattern becomes organized and orderly especially when, as in the rat, this happens by taking away DPOAEs.

It also seems unlikely that suppression of the primaries by the 1/3-oct IT leading to a decrease in DPOAEs could be mistaken for basal sources. In the preset study there were several situations where DP-grams with and without the IT were nearly equivalent [for example, the human (Fig. 1-A2) and rat (Fig. 3-A2)], which would not be expected if the IT suppressed f_2. Similar outcomes were previously observed for the rabbit (see Fig. 3, Martin *et al*., 2010a) where DP-grams collected with and without the 1/3-oct IT were equivalent in level, and still were accompanied by large residuals most likely representing basal DPOAE components. Thus, when DP-grams or DPOAE L/P maps were decreased in level by the 1/3-oct IT, this decrease likely represented the removal of substantial basal emissions that were previously contributing to the overall level of the DPOAE.

Finally, there is ample evidence for basal DPOAE sources in the literature (reviewed in Martin *et al*., 2010a) based upon DPOAE suppression tuning curves (Martin *et al*., 1999, 2003; Howard *et al*., 2002, 2003), DPOAE onset latencies (Whitehead *et al*., 1996; Cone *et al*., 2009), and noise over-exposures (Avan *et al*., 1991, 1995, 1997) to name a few examples. In view of the results of prior studies, the demonstration of basal DPOAE components is not particularly surprising. However, the consistency of the findings across the four species of the present study makes the claim that substantial basal DPOAE components contribute to the overall DPOAE a more universal and coherent hypothesis.

Perplexingly, these DPOAE components have two different phase behaviors previously thought to be attributable primarily to reflection from the f_{dp} (steep phase slopes/vertical phase banding) or distortion at f_2 (shallow phase slopes/horizontal phase banding). This apparent mixture of components can clearly be seen in humans (e.g., Fig. 1-C6) and rats (e.g., Fig. 4-C6). In the case of human DPOAEs, it seems well-established (e.g., Shera and Guinan, 1999; Talmadge *et al*., 1999; Kalluri and Shera, 2001; Konrad-Martin *et al*., 2001, 2002; Abdala and Dhar, 2010) that two mechanisms, namely distortion emanating from near f_2 and reflection from regions near f_{dp}, can explain the different phase behaviors. However, recent findings (Martin *et al*., 2009, 2010a,b), along with the present results, indicate that DPOAE components with steep or shallow phase gradients can derive from BM regions significantly above f_2. There could be a separate mechanism apart from reflection to account for the steep phase gradient DPOAEs, or there may be other reasons that these DPOAEs assume this phase behavior.

Based upon the sum of our experience, we hypothesize that basal DPOAE components represent distributed sources generated by input to the OHC nonlinearities all along the portion of the cochlea where the f_1 and f_2 TW tails overlap. The size of the basal sources at any particular frequency place that can be removed by the IT seem to be generally proportional to the amount of overlap of the TWs, thus, they get larger as they approach the peak of the f_2 TW, where overlap is maximal generally near f_2 (Martin *et al*., 2010a,b). Indeed, there may be no clear demarcation between basal distortion sources and distortion sources near f_2. Thus, we are operationally defining basal sources as those that can be influenced by a 1/3-oct IT. The shallow phase slopes of distortion components is thought to largely be the result of cochlear-scaling symmetry (Zweig and Shera, 1995; Shera and Guinan, 1999). Due to this property, as f_1 and f_2 are swept, the number of wavelengths within the cochlea remains constant. If it assumed that the

region of emission generation scales with the primaries then the measured phase of the DPOAE remains relatively constant as well. However, if this scaling assumption is violated, then it cannot be assumed that DPOAE components generated by nonlinear distortion will have shallow phase gradients. While basal DPOAE components are probably distortion components, their region of generation's relationship to cochlear scaling likely controls the phase characteristics of these emissions. If the region of generation is constrained in such a way that it can no longer scale with the input stimuli, then the phase can assume a place-fixed (steep phase gradient) behavior. One example of this situation appears to occur in the extreme apex of the cochlea. Here, cochlear scaling apparently breaks down and horizontal banding assumes a curvature and, in some cases, becomes vertical. This effect is apparent in the apical portion of the phase maps for all four species. In extreme cases such as the rat (Fig. 4-C2), and at high f_2/f_1 ratios and low frequencies for humans (Meinke *et al.*, 2006), DPOAEs can no longer be generated in the extreme apex and these DPOAEs apparently come from a region basal to their f_2 frequency place.

The above considerations are interesting in view of the recent efforts of Shera and colleagues (Shera and Guinan, 2003; Shera *et al.*, 2000, 2008, 2010) to measure cochlear tuning using stimulus frequency otoacoustic emissions (SFOAEs). These investigators give considerable discussion to the "significance of the apical–basal transition" where cochlear mechanics appear to differ between the apex vs the base, and a transition occurs between scaling and non-scaling behavior. Based upon the phase changes in the DPOAE L/P maps, this occurs generally around 4 kHz in chinchillas and rats, and at lower frequencies for rabbits and humans. In the Shera *et al.* (2010) data, a "short-latency SFOAE becomes significant" in this apical-like zone. The present data suggest that in this area emission components can arise almost entirely basal to the peak of f_2. This observation is consistent with and may in part explain some of the unusual behavior, such as short-latency SFOAEs, described for various cochlear measures obtained from this non-scaling region.

Another factor that appears to control the phase behavior of DPOAEs is some type of "constraint" that causes them to arise from a relatively fixed location as the primary-tones are swept in frequency. Thus, the place-fixed phase behavior of the $2f_2-f_1$ DPOAE likely arises because components generated apical to the $2f_2-f_1$ frequency place cannot travel past the $2f_2-f_1$ frequency place on the BM without being absorbed. Consequently, the measured DPOAE exhibits vertical phase banding behavior in DPOAE L/P maps, because its generation site is "constrained" to a region above the $2f_2-f_1$ DPOAE frequency place as the primaries are swept. Similar effects can occur when the cochlea is damaged. In such a situation, basal DPOAEs generated in the tails of the TWs can only come from a region where the OHCs are functioning normally. This effect can be seen in a noise-damaged rabbit ear (see Fig. 8 in Martin *et al.*, 2010a) where DPOAE phase appears very similar to that observed in the cochlear apex, but in this instance, it occurs near the basal edge (low-frequency end of the normal region) of an area exhibiting severe low-frequency cochlear damage.

A more difficult problem is trying to understand why narrow f_2/f_1-ratio $2f_1-f_2$ DPOAEs would exhibit place-fixed phase characteristics. A clue to unraveling this problem may be to assume that the narrow-ratio DPOAEs observed in the ear canal are not lower-sideband DPOAEs generated near f_2 as might be expected. Rather, they are DPOAEs generated in the same basal nonlinearities responsible for the $2f_2-f_1$ DPOAEs. This notion could explain why narrow f_2/f_1-ratio $2f_1-f_2$ DPOAE features such as magnitude notches and phase patterns are always contiguous with $2f_2-f_1$ DPOAEs in DPOAE L/P maps. Data in noise-damaged rabbits where wide f_2/f_1-ratio $2f_1-f_2$ DPOAEs tracked the damage pattern, but narrow-ratio $2f_1-f_2$ DPOAEs did not (Stagner *et al.*, 2005), are consistent with this view, and suggests that narrow- and wide-ratio $2f_1-f_2$ emissions do not come from the same place on the BM. The narrow-ratio $2f_1-f_2$ DPOAE may assume the place-fixed phase behavior of the $2f_2-f_1$ DPOAE because the close proximity of the primaries at these narrow ratios completely suppresses the $2f_1-f_2$ DPOAE normally generated near f_2, and constrains the basal generation region of the $2f_1-f_2$ DPOAE to a region near that of the $2f_2-f_1$ DPOAE. One advantage of all of the above suggestions is that a new emission generation mechanism does not need to be proposed to explain instances of reflection-like emissions arising basal to f_2.

Regardless of the mechanism of generation, it appears that both humans and some common laboratory species have DPOAEs generated basal to the 1/3-oct IT that can assume reflection- or distortion-like phase patterns. Consequently, the commonly accepted two-source model of DPOAEs may need modification to account for, or to include, the presence of these additional sources of emissions likely to be generated by nonlinear distortion, but capable of assuming two types of phase behavior. Clearly, phase behavior alone cannot be assumed to be a unique signature of emissions generated near the f_{dp} or f_2. Past evidence for basal DPOAE components (Martin *et al.*, 2010a) relied heavily upon results obtained from the ears of normal and noise-damaged rabbits. The present study extends these outcomes to chinchillas and rats exhibiting normal cochlear function, and suggests that the generation of DPOAEs as a distributed source basal to f_2 is a general phenomenon across a variety of species.

ACKNOWLEDGMENTS

This work was supported by the VA Loma Linda Healthcare System and by grants from NIH (DC000613) and the Veterans Administration (VA/RR and D C449R, C6212L). The authors thank Alisa Nelson-Miller for technical assistance and Dr. Laurence D. Fechter and Caroline Gearhart for help in measuring DPOAEs in rats. The authors also thank Dr. Paul F. Fahey and three anonymous reviewers for their helpful comments on the manuscript.

Abdala, C., and Dhar, S. (**2010**). "Distortion-product otoacoustic emission phase and component analysis in human newborns," J. Acoust. Soc. Am. **127**, 316–325.

Avan, P., Bonfils, P., Loth, D., Elbez, M., and Erminy, M. (**1995**). "Transient-evoked otoacoustic emissions and high-frequency acoustic trauma in the guinea pig," J. Acoust. Soc. Am. **97**, 3012–3020.

Avan, P., Bonfils, P., Loth, D., Narcy, P., and Trotoux. J. (**1991**). "Quantitative assessment of human cochlear function by evoked otoacoustic emissions," Hear. Res. **52**, 99–112.

Avan, P., Elbez, M., and Bonfils, P. (**1997**). "Click-evoked otoacoustic emissions and the influence of high-frequency hearing losses in humans," J. Acoust. Soc. Am. **101**, 2771–2777.

Cone, B., Martin, G. K., Stagner, B. B., and Lonsbury-Martin, B. L. (**2009**). "DPOAE-onset vs ABR latencies demonstrate fast DPOAE reverse travel times," Am. Audit. Soc. Bull. **34**, 44.

Dhar, S., Long, G. R., Talmadge, C. L., and Tubis, A. (**2005**). "The effect of stimulus-frequency ratio on distortion product otoacoustic emission components," J. Acoust. Soc. Am. **117**, 3766–3776.

Fahey, P. F., Stagner, B. B., Lonsbury-Martin, B. L., and Martin, G. K. (**2000**). "Nonlinear interactions that could explain distortion product interference response areas," J. Acoust. Soc. Am. **108**, 1786–1802.

Howard, M. A., Stagner, B. B., Lonsbury-Martin, B. L., and Martin, G. K. (**2002**). "Effects of reversible noise exposure on the suppression tuning of rabbit distortion-product otoacoustic emissions," J. Acoust. Soc. Am. **111**, 285–296.

Howard, M. A., Stagner, B. B., Foster, P. K., Lonsbury-Martin, B. L., and Martin, G. K. (**2003**). "Suppression tuning in noise-exposed rabbits," J. Acoust. Soc. Am. **114**, 279–293.

Kalluri, R., and Shera, C. A. (**2001**). "Distortion-product source unmixing: A test of the two-mechanism model for DPOAE generation," J. Acoust. Soc. Am. **109**, 622–637.

Knight, R. D., and Kemp, D. T. (**2000**). "Indications of different distortion product otoacoustic emission mechanisms from a detailed f_1,f_2 area study," J. Acoust. Soc. Am. **107**, 457–473.

Knight, R. D., and Kemp, D. T. (**2001**). "Wave and place fixed DPOAE maps of the human ear," J. Acoust. Soc. Am. **109**, 1513–1525.

Konrad-Martin, D., Neely, S. T., Keefe, D. H., Dorn, P. A., and Gorga, M. P. (**2001**). "Sources of distortion product otoacoustic emissions revealed by suppression experiments and inverse fast Fourier transforms in normal ears," J. Acoust. Soc. Am. **109**, 2862–2879.

Konrad-Martin, D., Neely, S. T., Keefe, D. H., Dorn, P. A., Cyr, E., and Gorga, M. P. (**2002**). "Sources of DPOAEs revealed by suppression experiments, inverse fast Fourier transforms, and SFOAEs in impaired ears," J. Acoust. Soc. Am. **111**, 1800–1809.

Martin, G. K., Stagner, B. B., and Lonsbury-Martin, B. L. (**2010a**). "Evidence for basal distortion-product otoacoustic emission components," J. Acoust. Soc. Am. **127**, 2955–2972.

Martin, G. K., Stagner, B. B., Chung, Y.-S., and Lonsbury-Martin, B. L. (**2010b**) "Systematic effects of interference tones presented above f2 on DPOAE residuals," 47th Inner Ear Biology Workshop: http://www.biomed.cas.cz/ieb/programme.html (p40) (last viewed 26 February 2011).

Martin, G. K., Stagner, B. B., Fahey, P. F., and Lonsbury-Martin, B. L. (**2009**). "Human steep and shallow DPOAE phase gradients not arising from DPOAE or f_2 frequency place," J. Acoust. Soc. Am. **125**, EL85–92.

Martin, G. K., Villasuso, E. I., Stagner, B. B., and Lonsbury-Martin, B. L. (**2003**). "Suppression and enhancement of distortion-product otoacoustic emissions by interference tones above f_2: II. Findings in humans," Hear. Res. **177**, 111–122.

Martin, G. K., Jassir, D., Stagner, B. B., Whitehead, M. L., and Lonsbury-Martin, B. L. (**1998**). "Locus of generation for the $2f_1$-f_2 vs $2f_2$-f_1 distortion product otoacoustic emissions in normal-hearing humans revealed by suppression tuning, onset latencies, and amplitude correlations," J. Acoust. Soc. Am. **103**, 1957–1971.

Martin, G. K., Stagner, B. B., Jassir, D., Telischi, F. F., and Lonsbury-Martin, B. L. (**1999**). "Suppression and enhancement of distortion-product otoacoustic emissions by interference tones above f_2. I. Basic findings in rabbits," Hear. Res. **136**, 105–123.

Martin, G. K., Lonsbury-Martin, B. L., Probst, R., Scheinin,, S. A., and Coats, A. C. (**1987**). "Acoustic distortion products in rabbit ear canal. II. Sites of origin revealed by suppression contours and pure-tone exposures,," Hear. Res. **28**, 191–208.

Meinke, D., Martin, G., and Stagner. B. (**2006**). "A harmonic difference-tone component in low-frequency human DPOAEs," Assoc. Res. Otolaryngol. Abstr 1152 .

Mills, D. M. (**1998**). "Interpretation of distortion product otoacoustic emission measurements. II. Estimating tuning characteristics using three stimulus tones," J. Acoust. Soc. Am. **103**, 507–523.

Shera, C. A., and Guinan, J. J., Jr. (**1999**). "Evoked otoacoustic emissions arise by two fundamentally different mechanisms: A taxonomy for mammalian OAEs," J. Acoust. Soc. Am. **105**, 782–798.

Shera, C. A., and Guinan, J. J., Jr. (**2003**). "Stimulus-frequency-emission group delay: A test of coherent reflection filtering and a window on cochlear tuning," J. Acoust. Soc. Am. **113**, 2762–2772.

Shera, C. A., Guinan, J. J., Jr., and Oxenham, A. J. (**2010**). "Otoacoustic estimation of cochlear tuning: Validation in the chinchilla," J. Assoc. Res. Otolaryngol. **3**, 343–365.

Shera, C. A., Talmadge, C. L., and Tubis, A. (**2000**). "Interrelations among distortion-product phase gradient delays: Their connection to scaling symmetry and its breaking," J. Acoust. Soc. Am. **108**, 2933–2948.

Shera, C. A., Tubis, A., and Talmadge, C. L. (**2008**). "Testing coherent reflection in chinchilla: Auditory-nerve responses predict stimulus-frequency emissions," J. Acoust. Soc. Am. **124**, 381–395.

Stagner, B. B., Nemanov, L. S., Martin, G. K., and Lonsbury-Martin, B. L. (**2005**) "Growth of response areas for lower- and upper-sideband DPOAEs measured at three f_2/f_1 ratios in normal and noise-exposed rabbits," Assoc. Res. Otolaryngol. Abstr. 943.

Talmadge, C. L., Long, G. R., Tubis, A., and Dhar, S. (**1999**). "Experimental confirmation of the two-source interference model for the fine structure of distortion product otoacoustic emissions," J. Acoust. Soc. Am. **105**, 275–292.

Whitehead, M. L., Stagner, B. B., Martin, G. K., and Lonsbury-Martin, B. L. (**1996**). "Visualization of the onset of distortion-product otoacoustic emissions, and measurement of their latency," J. Acoust. Soc. Am. **100**, 1663–1679.

Zweig, G., and Shera, C. A. (**1995**). "The origin of periodicity in the spectrum of evoked otoacoustic emissions," J. Acoust. Soc. Am. **98**, 2018–2047.